

Selenomethionine phasing from MAD data collected with the **mar555** flatpanel detector

Claudio Klein, Marresearch GmbH, Norderstedt

Introduction

Selenium is one of the few materials capable of converting X-rays directly into electrons. The *mar555* flatpanel detector makes use of this unique property of selenium. With its highly sophisticated read-out system, the detector directly counts the X-rays where they hit the detector without taking the detour of converting them into visible light as other detectors like the CCD's and image plate scanners do. The result of this direct conversion is an unprecedented spatial resolution and improved signal-to-noise ratio.

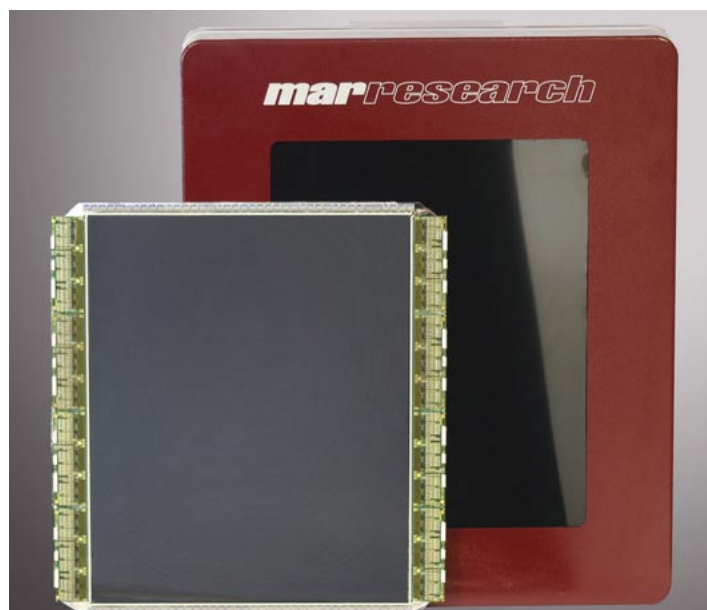
It has been argued, though, that X-rays with energies around the Se K absorption edge (0.9795 Ang.) may have a significant impact on the performance of this Se-coated detector. Selenomethionine phasing techniques have become an important tool in protein crystallography. Therefore any new detector technology will have to prove that it can be used for MAD phasing of selenated proteins.

In this study, we have used a *mar555* detector system to collect MAD data around the Se K edge. As test case, we used a frozen crystal of the feruloyl esterase domain of Xylanase10B (FAE). All data were collected at ESRF beamline ID23-1.

Experiment

X-ray Detector System

Detector	<i>mar555</i>
Read-out time	1.25 sec
Active area	430 mm x 350 mm
Diagonal	555 mm
Pixel size	139 μ
Total number of pixels	2560 x 3072
Dynamic range	0 - 250.000
Total noise	750 e rms (= 6 X-rays @ 12 keV)



Crystal

Protein	Feruloyl esterase domain of Xylanase 10B ¹
PDB entry	1GKK ¹
Space group	P 2 ₁ 2 ₁ 2 ₁
Unit cell parameters	a=65.4 b=108.8 c=113.9
Amino acid residues	2 x 296 (dimer)
Anomalous scatterers	2 x 8 seleniums in methionines 2 x 5 Cd ions from crystallization buffer 2 x 1 phosphate ion from phosphorylated Ser
Size of crystal	1000 μ x 100 μ x 50 μ
Mosaicity	< 0.1°

Data collection

System	<i>mar555</i> @ ESRF ID23-1
Distance	210 mm
Exposure time	0.3 sec / 1.0 deg.
Transmission	40 %
Energy	12.650, 12.656, 12.680 keV
Total no. of images	135 at each energy
Multiplicity	2.88
High resolution limit	1.8 Ang.

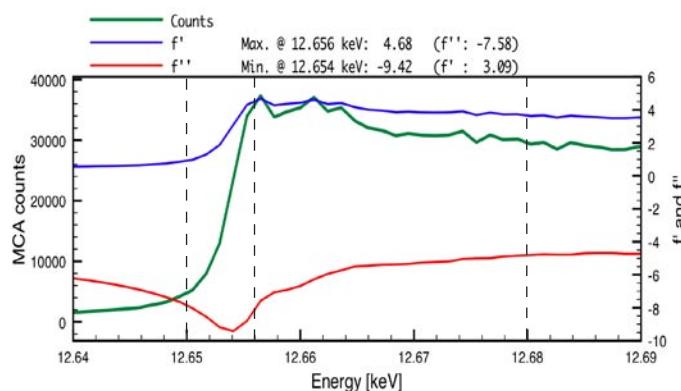


Figure 2: Energy scan

The dotted vertical lines show the selected energies of 12.650 keV (low remote), 12.656 keV (peak) and 12.680 keV (high remote).

Data processing (XDS²)

Energy	12.650 low remote	12.656 peak	12.680 high remote
R_{merge}	4.0 (9.5)	5.0 (19.2)	5.5 (19.8)
R_{meas}	5.0 (11.7)	6.2 (23.6)	6.8 (24.3)
$\text{Sig}_{\text{ano}}(\text{XDS})$	1.09 (0.93)	1.70 (1.05)	1.43 (1.01)
$\langle I/\sigma \rangle$	20.5 (11.1)	17.2 (6.7)	17.2 (7.3)
Completeness	97.6 (96.7)	97.6 (96.8)	97.7 (96.7)
Measurements	409281	407632	411896
Unique hkl	142010	141991	142264
Multiplicity	2.88	2.87	2.89

Last shell (1.92-1.80 Ang.) in parentheses

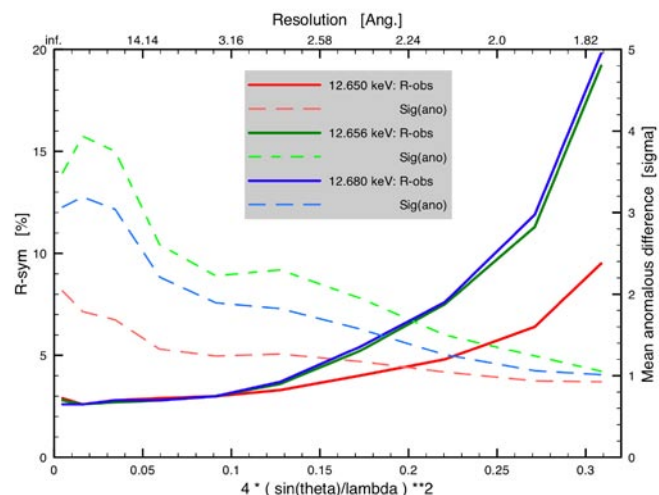


Figure 3: R-factors and anomalous signals

The dotted lines show SigAno values as computed by XDS.

Structure solution and phasing

The data sets of 3 energies were merged to give combined intensities. Program SHELXD^{3,4,5,6} was instructed to locate 26 anomalous scatterers: 16 seleniums and 10 Cd ions.

SHELXD located all of them. The best solution was used for phase calculation and further improvement by density modifications and phase extension to 1.2 Ang. ("free lunch algorithm") with program SHELXE⁶. The automatic tracing of the final experimental map shown in Figure 5 is very straightforward. It does not differ much from the density of the final model.

SHELXD

High resolution limit	2.0 Ang.
CC all / weak	44.26 / 10.90
PATFOM	5.04
No. of located peaks	26

SHELXE

High resolution limit	1.20 Ang.
No. of cycles	400
Contrast (enantiomorph)	0.312 (0.101)
Connectivity (enantiomorph)	0.828 (0.863)
Pseudo-free CC (enantiomorph)	81.86 (28.63) %

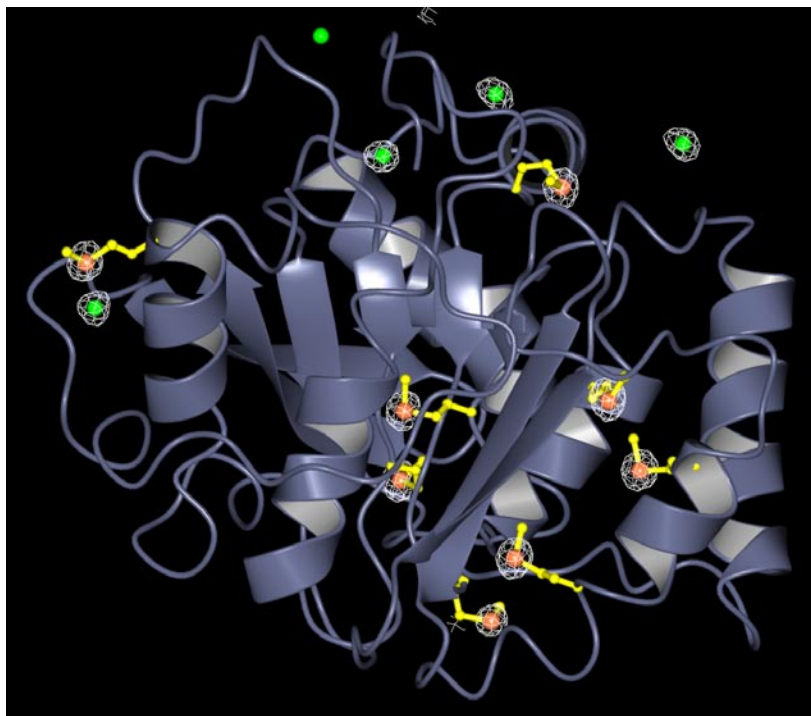
Figure 4: Anomalous difference Fourier map

The phases for the map are from the refined model. The map shows all density $> +4 \sigma$ (white). Cd ions are drawn in green, Se atoms in coral and methionine residues in yellow.

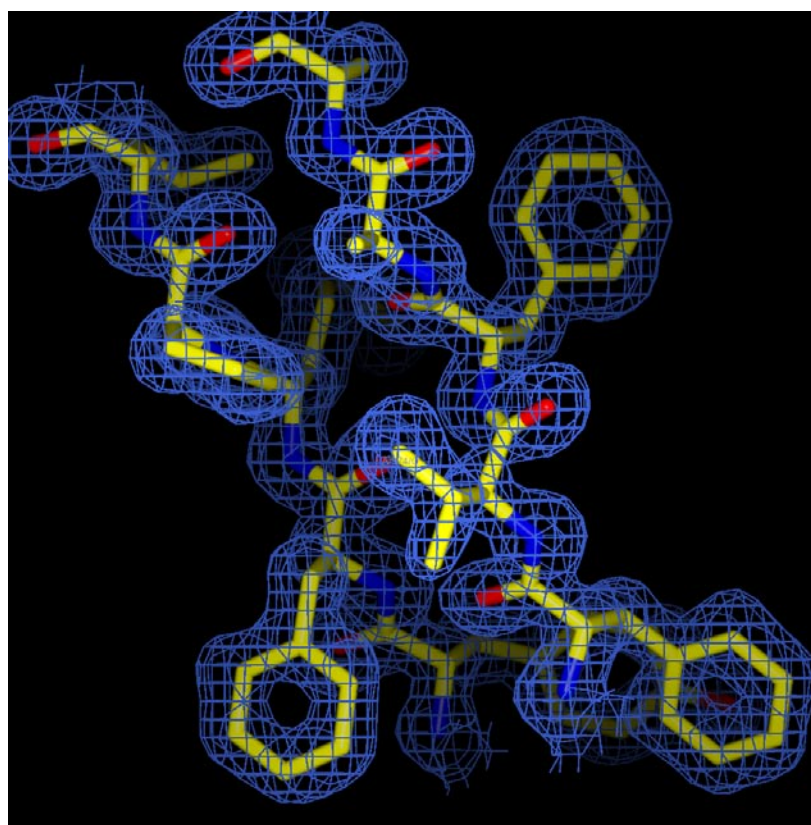
For sake of clarity, only molecule A of the dimer is shown.

The 3 highest peak in the map are:

- 1.) MSE 964 Se : 33.9 σ
- 2.) Cd 2089: 21.4 σ
- 3.) MSE 955 Se: 20.5 σ

**Figure 5: Experimental map**

The phases for the map are from 26 Se positions after density modifications and phase expansion to 1.2 Ang. by SHELXE. A typical section of the map shows residues ranges 973 to 977 and 1009 to 1013 located in the central beta-sheet. Contours are drawn at 1.1 σ .



Phasing from SAD data

Each individual data set can be used for SAD phasing. The structure solution follows the same pattern as for the combined data from 3 energies and produces an experimental map that allows for full chain tracing and automatic model building. In addition to the data collected around the Se absorption edge, further data were collected at lower energy (7keV= 1.77 Ang. and 6keV = 2.01 Ang.). While the obtained resolution was restricted to 2.4 Ang. and 2.7 Ang., respectively, SAD phases can readily be obtained that again produce traceable maps (data not shown here).

Conclusion

The MAD data from the *mar555* flatpanel detector yield protein phases of impressive quality. This is despite the relatively low multiplicity of each data set (approx. 3). The data collected with energies above and below the Se absorption edge behave very similarly and do not reveal any particular problems like absorption effects of the selenium-coating of the detector.

Acknowledgements:

We would like to thank the staff of the ESRF, namely Dr. Didier Nurizzo, Dr. Sean McSweeney and Dr. Gordon Leonard, for provision of FAE crystals and data collection facilities and their excellent beamline support.

References:

1. Prates, J.A.M., Tarbouriech, N., Charnock, S.J., Fontes, C.M.G.A., Ferreira, L.M.A., & Davies, G.J. (2001). *Structure*, **9**, 1183–1190.
2. Kabsch, W. (1993). *J. Appl. Cryst.* **26**, 795-800.
3. Sheldrick, G. M., Hauptman, H. A., Weeks, C. M., Miller R. & Us—n I. (2001), *International Tables F*, edited by E.Arnold & M.Rossmann, pp. 333-351. Dordrecht: Kluwer Academic Publishers
4. Schneider, T.R. & Sheldrick, G.M. (2002) *Acta Cryst.* **D58**, 1722-1779
5. Uson, I. & Sheldrick, G.M. (1999). *Curr.Opin. Struct.Biol.* **9**, 643-648
6. Sheldrick, G.M. (2002). *Z. Kristallogr.* **217**, 644650